sustainability

MDPI

Article

Prediction of the Tunnel Collapse Probability Using SVR-Based Monte Carlo Simulation: A Case Study

Guowang Meng [1,2], Hongle Li [1,2], Bo Wu [1,3,*], Guangyang Liu [1,2], Huazheng Ye [1] and Yiming Zuo [1]

1 School of Civil Engineering and Architecture, Guangxi University, 100 University Road, Nanning 530004, China
2 State Key Laboratory of Featured Metal Materials and Life-Cycle Safety for Composite Structures, Guangxi University, Nanning 530004, China
3 School of Civil and Architectural Engineering, East China University of Technology, Nanchang 330013, China
* Correspondence: wubo@ecut.edu.cn

Abstract: Collapse is one of the most significant geological hazards in mountain tunnel construction, and it is crucial to accurately predict the collapse probability. By introducing the reliability theory, this paper proposes a calculation method for the collapse probability in mountain tunnel construction based on numerical simulation, support vector regression (SVR), and the Monte Carlo (MC) method. Taking the Jinzhupa Tunnel Project in Fujian Province as a case study, three-dimensional models were constructed, and the safety factors of the surrounding rock were determined using the strength reduction method. By defining the shear strength parameters of the surrounding rock as random variables, the problem was formulated as a reliability model, and the safety factor was chosen as the reliability index. To increase computational efficiency, the SVR model was trained to replace numerical simulations, and the MC method was adopted to calculate the probability of collapse. The results showed that the cause of the collapse was the change in the excavation method and the very late installation of supports. The feasibility and reliability of the proposed method have been verified, indicating that the method can be used to predict the probability of collapse in a practical risk assessment of mountain tunnel construction.

Keywords: mountain tunnel; collapse risk assessment; support vector regression; Monte Carlo method; reliability theory

Citation: Meng, G.; Li, H.; Wu, B.; Liu, G.; Ye, H.; Zuo, Y. Prediction of the Tunnel Collapse Probability Using SVR-Based Monte Carlo Simulation: A Case Study. *Sustainability* **2023**, *15*, 7098. https://doi.org/10.3390/su15097098

Academic Editor: Jianjun Ma

Received: 15 March 2023
Revised: 11 April 2023
Accepted: 20 April 2023
Published: 24 April 2023

1. Introduction

China has the largest number and the fastest development rate of highway tunnels in the world [1]. Complex geological conditions are inevitably encountered in mountain tunnel construction, resulting in frequent geological hazards. Wang et al. [2] reported 97 geological hazard accidents in mountain tunnel construction in China between 2002 and 2018, resulting in 393 fatalities, 467 injuries, and 51 missing. According to the report, the collapse was the most common form of geological hazard, accounting for 62.89 percent. Therefore, a more accurate and effective evaluation of the collapse risk in mountain tunnels is of crucial practical importance.

Over the past decade, a great deal of research has been conducted in the risk assessment of tunnel collapse. Ou et al. [3] proposed a new risk assessment method for tunnel collapse based on case analysis, advanced geological prediction, and Dempster–Shafer evidence theory. Xu et al. [4] proposed an attribute recognition model of loess tunnel collapse risk assessment, which is based on the attribute mathematical theory. Sharafat et al. [5] proposed a novel risk analysis method based on the generic bow-tie method in order to simultaneously identify the risk causes and consequences of TBM tunneling projects in difficult ground conditions. To assess the probability of collapse, Sun et al. [6] proposed a novel assessment method based on multistate fuzzy Bayesian networks integrated with multiple features. Ou et al. [7] proposed a multistate dynamic Bayesian network (DBN) evaluation method for highway tunnel collapse based on parameter learning. Meanwhile, some studies used artificial intelligence algorithms for risk assessment to realize the automation and intelligence of the assessment process. In order to predict the occurrence of collapse hazards quickly, Li [8] developed a risk assessment model based on a support vector machine. Wu et al. [9] proposed a multisource information fusion assessment method for tunnel collapse using artificial intelligence, including the Gaussian process regression. The Gaussian process regression used in this method played a role in predicting the deformation of the surrounding rock in the next few days after the excavation.

On the one hand, previous research, with or without the use of artificial intelligence algorithms, typically selected and graded risk indicators based on engineering experience, resulting in subjective evaluation results. With the capability of taking numerous factors into account, such as nonlinear rock behavior, soil–structure interaction, and construction methods, numerical methods have proven to be an effective and realistic approach to analyzing the safety of tunnel construction [10,11]. Therefore, the introduction of numerical methods into the risk assessment process can effectively improve the reliability of the results [12]. On the other hand, the quantification of the collapse hazard probability, which is one of the main elements of risk assessment, has rarely been considered in previous studies, except for those based on Bayesian networks. Furthermore, few studies have assessed the collapse risk of tunnels under specific construction behaviors. Considering that the probability of tunnel collapse is influenced by numerous uncertainties, especially the uncertainty of the surrounding rock properties, the reliability-based method can be applied to the calculation [13]. The Monte Carlo (MC) method is one of the most popular and well-documented methods for reliability analysis; it calculates the exceedance probability for any desired reliability index in a target structure [14,15]. However, to ensure the accuracy of the calculation, the MC method requires a large number of random samples. Given the time required for numerical simulations, it may not be practical to perform MC simulations directly with numerical methods. Currently, machine- and deep-learning techniques are efficient tools for predicting tunnel performance [16,17], and support vector regression (SVR) is considered to increase computational efficiency in this study.

In order to probabilistically assess the collapse risk in mountain tunnels under specific construction behaviors, this paper adopts the reliability theory and proposes a novel method for predicting the collapse probability of mountain tunnels based on numerical simulation, support vector regression, and the Monte Carlo method. The proposed method can provide references for project managers to choose a safe excavation method and to develop reasonable construction schemes. The significant difference between this paper and similar studies [18,19] is that the proposed method adopts the safety factor of the surrounding rock as the random output parameter, and it adopts the reliability index instead of the deformation, which makes the proposed method more reliable because the modulus significantly affects the deformation, and the exact value of it is difficult to determine. As a case study, an overview of the Jinzhupa Tunnel of the Puyan Expressway in Fujian Province, China, was obtained, and a FLAC3D numerical model was constructed. Then, the strength reduction method, which provides an effective way to analyze the stability of tunnels, was implemented in the FLAC3D simulation to determine the safety factor of the surrounding rock. Next, based on the numerical results, the SVR model was trained to replace numerical simulations in order to increase computational efficiency. Finally, in conjunction with the well-trained SVR model, a sufficient number of random samples were used to calculate the collapse probability using the MC method.

2. Theory and Methodology

2.1. Strength Reduction Method and the Failure Criterion

The strength reduction method is widely used in stability analysis of slope. Some scholars in the tunnel field introduced the strength reduction method into the stability analysis of tunnels, and the corresponding achievements verified the applicability of the method to tunnel engineering [20–23]. For the surrounding rock described by the Mohr–

Coulomb yield criterion, the strength reduction method involves dividing the actual shear strength parameters c and φ by the strength reduction coefficient K:

$$c' = \frac{c}{K}, \varphi' = \arctan\left(\frac{\tan\varphi}{K}\right) \tag{1}$$

The actual shear strength parameters are then replaced with the new shear strength parameters c' and φ'. To obtain the factor of safety, the strength reduction coefficient (K) must be incrementally increased until the surrounding rock reaches its limit state. At this point, the safety factor is equal to the strength reduction coefficient, i.e., $F_s = K$.

When the strength reduction method is introduced into the numerical methods for stability analysis of tunnels, the resulting safety factor depends significantly on the failure criteria. Currently, three commonly used failure criteria for tunnels are the abrupt displacement criterion [24], the penetration of plastic yield zone criterion [25], and the numerical non-convergence criterion [20], which are the same for slope. In this paper, the abrupt displacement criterion was chosen for the stability analysis of the surrounding rock because of its high accuracy and clear physical significance [24]. The abrupt displacement criterion requires that the displacement of certain characteristic points should increase abruptly when the strength reduction coefficient (K) increases to a certain value. The inflection point of the curve between displacement and strength reduction coefficient is considered the limit state, and the corresponding strength reduction coefficient is equivalent to the safety factor of the surrounding rock.

According to the previous research [26,27], the safety factor of 1.30 was determined as the critical value for determining the stability of the surrounding rock by integrating various factors that cannot be considered by numerical simulation (such as overbreak, unfavorable geology, etc.), and it is believed that the tunnel is prone to collapse when the safety factor of the surrounding rock is less than 1.30.

2.2. Stress Release Method for Support Timing Control

The stress release method is often used to simulate the spatial effects of the excavation process, such as the simulation of the two-dimensional excavation support process, the formation pressure release and support pressure control process, and the three-dimensional support timing control process [28]. The stress release method of this study is based on the technique proposed by Duncan and Dunlop [29]. The method is implemented in FLAC3D by controlling the nodal unbalanced force at the excavation boundary (Figure 1). First, the initial state of the model is obtained by applying gravity (Figure 1a). Second, the null model is assigned to the zones to be excavated, representing the removal of rock from the model. The model is then solved for a single step, resulting in the generation of only the nodal unbalanced force at the excavation boundary (Figure 1b). Then, the nodal unbalanced force is reversed and multiplied by a certain coefficient, and the model is solved to the equilibrium state to achieve the desired release rate (Figure 1c). Finally, the support is installed after the nodal unbalanced force is removed (Figure 1d).

2.3. The Monte Carlo Method

The Monte Carlo method, also known as the random simulation method and the random sampling method, is often used to simulate random phenomena in engineering. In reliability analysis, the state of the random sample is determined by the limit state function, which is described as follows:

$$g(X) = f_0 - f(X) \tag{2}$$

where $f(X)$ is the performance function, and f_0 is the corresponding threshold.

If k times $g(X) < 0$ is obtained by N random calculations, the failure probability is given by

$$p_f = \frac{k}{N} \tag{3}$$

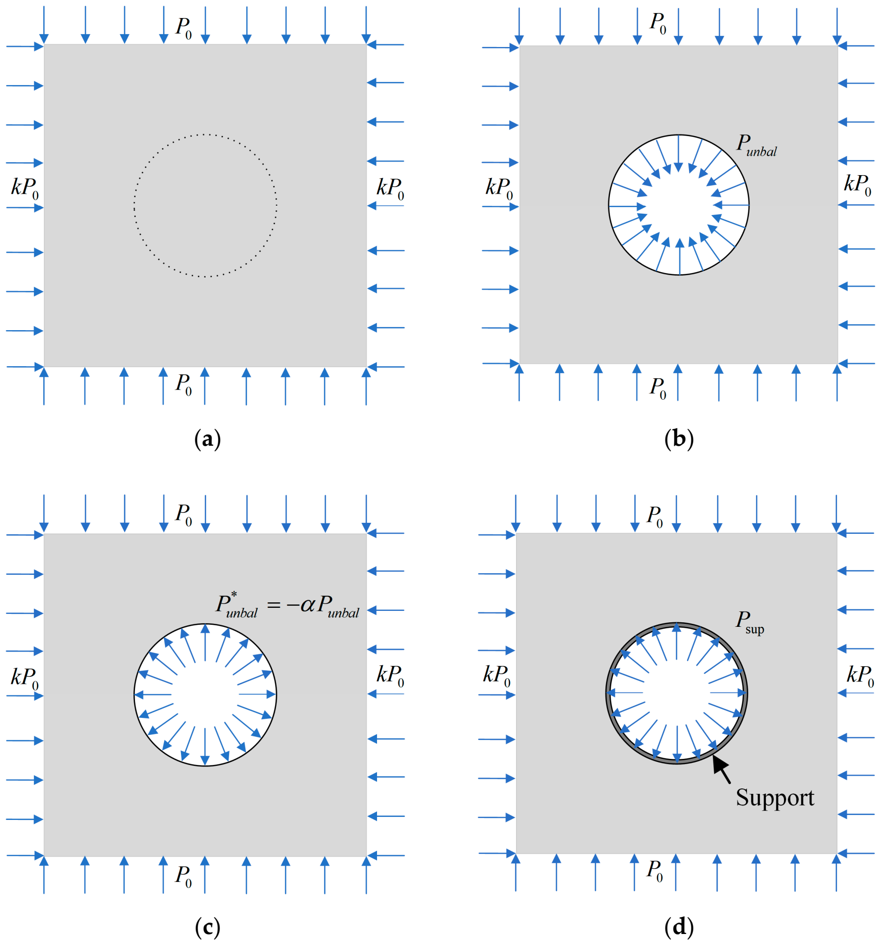

Figure 1. Simulation process for support timing control: (**a**) initial state; (**b**) generation of unbalanced force; (**c**) reverse of unbalanced force; (**d**) removal of unbalanced force and support installation.

2.4. Support Vector Regression

Support vector machines (SVMs), which were proposed by Vapnik et al. in 1995, are a widely used machine-learning method for classification, regression, and other learning tasks, with excellent performance in solving small sample and nonlinear problems [30]. The support vector machine for regression is briefly introduced in this section. Consider a set of training points, $\{(x_1, z_1), \ldots, (x_l, z_l)\}$, where $x_i \in R^n$ is a feature vector and $z_i \in R$ is the target output. Given a penalty factor C > 0 and an insensitive loss function ε > 0, the standard form of SVR [31] is

$$\min_{\omega,b,\xi,\xi^*} \frac{1}{2}\omega^T\omega + C\sum_{i=1}^{l}\xi_i + C\sum_{i=1}^{l}\xi_i^* \tag{4}$$

The constraint conditions are as follows:

$$\begin{cases} \omega^T\phi(x_i) + b - z_i \le \varepsilon + \xi_i, \\ z_i - \omega^T\phi(x_i) - b \le \varepsilon + \xi_i^*, \\ \xi_i, \xi_i^* \ge 0, i = 1, \ldots, l. \end{cases} \tag{5}$$

The dual problem is

$$\min_{\alpha,\alpha^*} \frac{1}{2}(\alpha - \alpha^*)^T Q(\alpha - \alpha^*) + \varepsilon\sum_{i=1}^{l}(\alpha_i + \alpha_i^*) + \sum_{i=1}^{l} z_i(\alpha_i - \alpha_i^*) \tag{6}$$

The constraint conditions are expressed in Equation (7):

$$\begin{cases} e^T(\alpha - \alpha^*) = 0, \\ 0 \leq \alpha_i, \alpha_i^* \leq C, i = 1, \ldots, l. \end{cases} \tag{7}$$

where $Q_{ij} = K(x_i, x_j) \equiv \phi(x_i)^T \phi(x_j)$.

After solving problem (6), the approximate function is

$$\sum_{i=1}^{l} (-\alpha_i + \alpha_i^*) K(x_i, x) + b \tag{8}$$

where $K(x_i, x_j)$ is the kernel function of SVM.

The performance of the SVR algorithm largely depends on the choice of kernel. Four commonly used kernel functions are listed as follows: linear kernel function, polynomial kernel function, radial basis function (RBF), and sigmoid function [32]. In this paper, RBF was selected as the kernel function for SVR models because of its excellent performance in practical applications [33].

2.5. Collapse Risk Prediction Method

The proposed method for predicting the collapse probability operates as follows:

(1) Several parameters are selected as random variables based on the actual conditions of the project. Then, a series of safety factors of the surrounding rock, derived from the FLAC3D simulations, are utilized as training data for SVR.
(2) The SVR model with ideal performance is obtained through the training process, and a nonlinear mapping between random variables and safety factors is established to replace the performance function of the Monte Carlo method.
(3) The reliability model for the problem is established and a limit state function is defined. Then, the number of random samples required for the MC method are determined to ensure probability convergence.
(4) The required number of random samples are generated and fed into a well-trained SVR model to execute the MC simulation. The number of random samples that fall into the failure domain is counted according to the limit state function, and the approximate failure probability, i.e., the collapse probability, can be obtained by Equation (3).

The flowchart of the proposed method is shown in Figure 2.

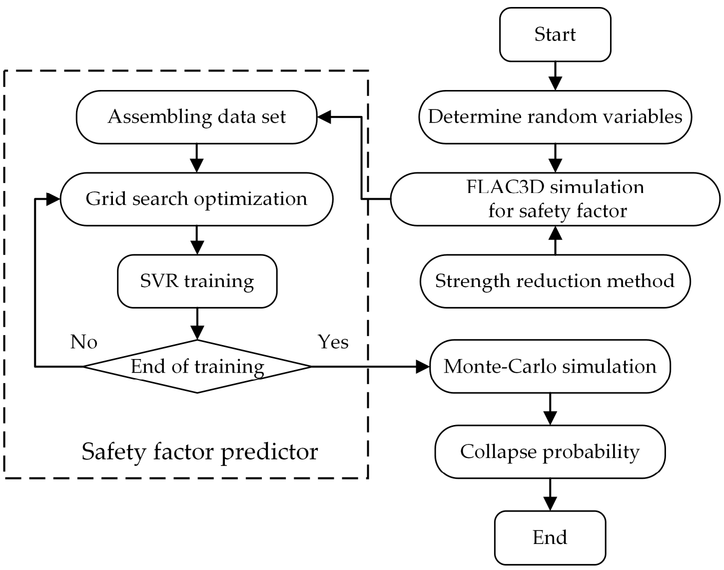

Figure 2. Flowchart of the proposed method.

3. Case Study

3.1. Overview of the Tunnel Excavation Project

The Jinzhupa Tunnel is a two-way six-lane tunnel located on the Puyan Expressway in Sanming City, Fujian Province, China (Figure 3). The site is covered with Quaternary slope residual soil, and the underlying bedrock consists of the Devonian sandstone and the Cambrian shale. Bedrock fracture water is the main groundwater type at this site. The maximum buried depth of the tunnel is 131 m. Figures 4 and 5 show the longitudinal geological profile of the Jinzhupa Left Tunnel and the design of the tunnel cross section, respectively. The exit of the left tunnel is in the direction of Jianning. The rock mass surrounding the tunnel exit is fractured and strongly weathered; it has poor self-stability and is prone to collapse during construction. Section A (ZK243 + 319~ZK243 + 279) and section B (ZK243 + 279~ZK243 + 245) were designed to be excavated using the twin-side heading method and the CRD method, respectively.

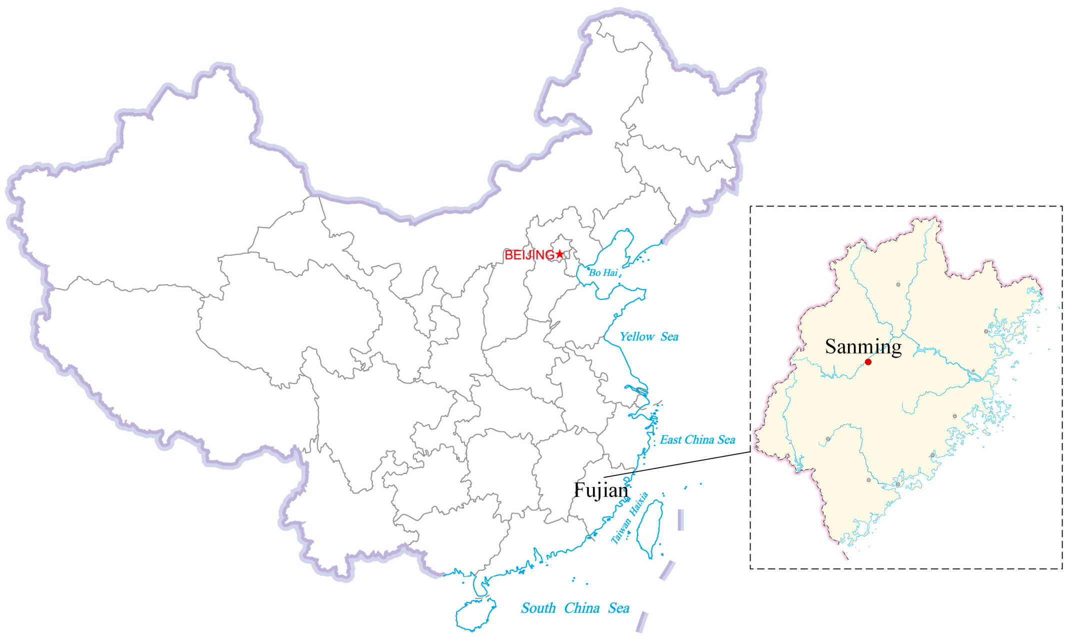

Figure 3. Location of the tunnel.

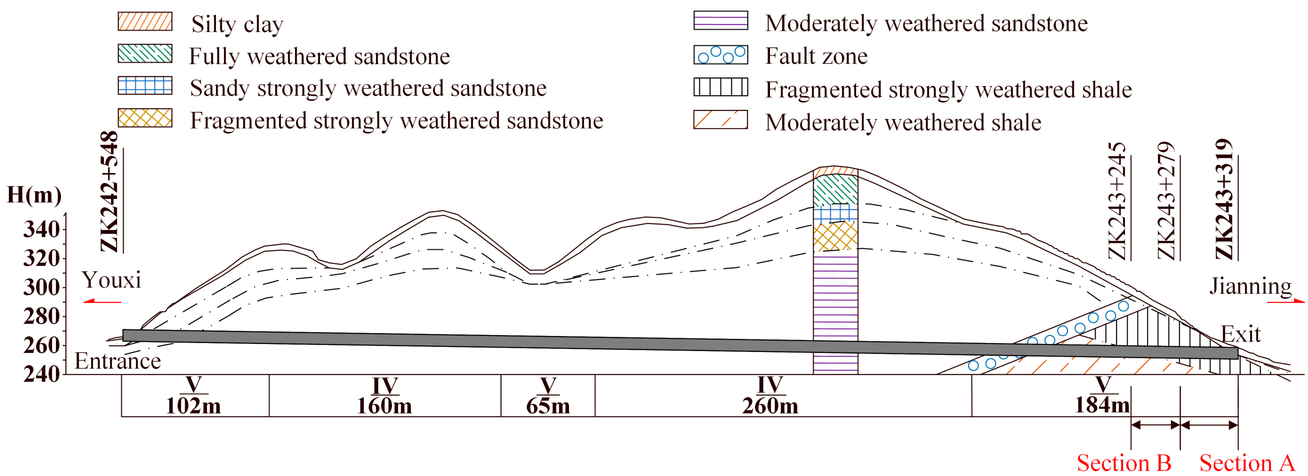

Figure 4. Longitudinal geological profile of the Jinzhupa Left Tunnel.

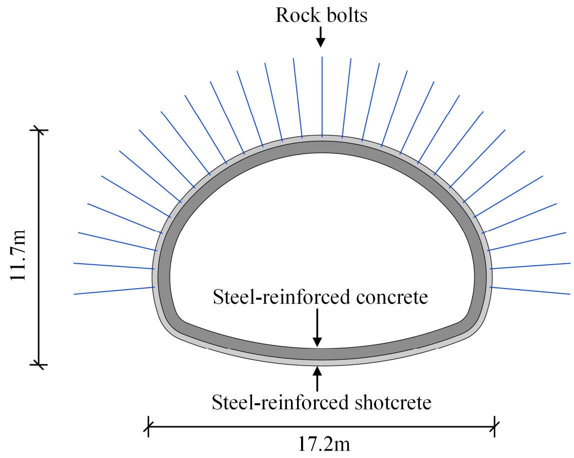

Figure 5. Cross section of the Jinzhupa Left Tunnel.

3.2. Numerical Modeling and Validation

Because the left tunnel was excavated 50 m ahead of the right tunnel, a 3D numerical model of the left tunnel was constructed in FLAC3D without the right tunnel (Figure 6). The dimensions of the model are X × Y × Z = 110 m × 70 m × 60 m, and the tunnel cross section has a width of 17.2 m and a height of 11.7 m. The tunnel passes through stratum I, which consists of fragmented, highly weathered shale. Stratum II consists of moderately weathered shale. The bottom and the side surfaces of the model were constrained in the normal direction, while the top surface was free. The mass of the silty clay at the surface and the change of longitudinal ground elevation were applied to the top surface by means of equivalent stress in the vertical direction. The density of the silty clay was 1840 kg/m^3 and the thickness was 3 m. The change of longitudinal ground elevation was 24.6 m. Hence, the equivalent vertical stress applied to each node on the top surface was −(55,200 + 8080y) Pa, where the value 55,200 Pa represented the gravity stress of the silty clay, and y was the y-axis position of the node. The following assumptions were made in the modeling process: (1) Since the groundwater level in the area was low and the tunnel was excavated during a dry winter, the effect of water was not considered. (2) The surrounding rock was an isotropic and continuous elastoplastic material described by the Mohr–Coulomb yield criterion. (3) The pipe shed, steel-reinforced shotcrete, and rock bolts were modeled using beam elements, shell elements, and cable elements, respectively, as isotropic and continuous plastic materials. Tables 1 and 2 list the properties of the rock and the primary support system, respectively.

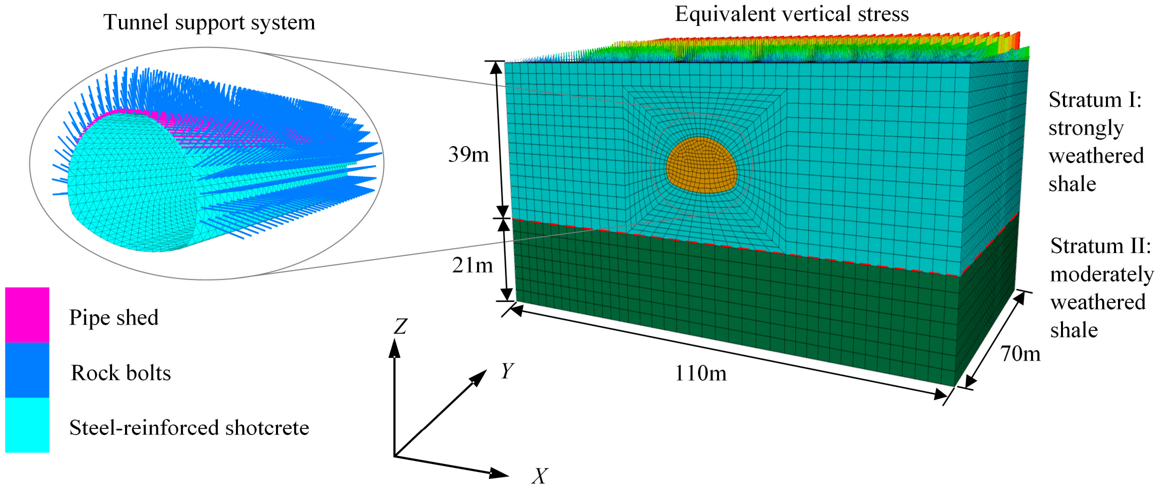

Figure 6. Three-dimensional view of the numerical model and tunnel support system.

Table 1. Rock properties of two strata.

Rock Type	Density (kg/m^3)	Elastic Modulus (GPa)	Poisson's Ratio	Bulk Modulus (GPa)	Shear Modulus (GPa)	Cohesion (kPa)	Friction Angle (°)
Stratum I	2300	0.2	0.35	0.22	0.06	10	30
Stratum II	2500	1.3	0.39	1.97	0.37	120	35

Table 2. Material properties of the support system.

Rock Bolts		Pipe Shed		Steel-Reinforced Shotcrete	
Parameter	Value	Parameter	Value	Parameter	Value
Density (kg/m^3)	7800	Density (kg/m^3)	7800	Density (kg/m^3)	2400
Elastic modulus (GPa)	210	Elastic modulus (GPa)	210	Elastic modulus (GPa)	30 (28 *)
Grout exposed perimeter (m)	0.3	Poisson's ratio	0.3	Poisson's ratio	0.25
Cross-sectional area (m^2)	4.233×10^{-4}	Cross-sectional area (m^2)	1.923×10^{-3}	Thickness (m)	0.28 (0.16 *)
Tensile yield strength (kN)	150	—	—	—	—
Grout cohesive strength (kPa)	200	—	—	—	—
Grout friction angel (°)	25	—	—	—	—
Grout stiffness (MPa)	17.5	—	—	—	—

* Note: Parenthesized values are intended for temporary steel-reinforced shotcrete.

According to the documentation provided by the project manager, the excavation and support installation of section A were completed. Therefore, FLAC3D simulations were performed according to the excavation sequence shown in Figure 7. The vertical displacement contour of the longitudinal section is shown in Figure 8a, and the comparison between simulation values and monitoring values of the vault settlement is shown in Figure 8b. It can be observed that the trend of the simulation values is similar to that of the monitoring values. In addition, the monitoring cross section and displacement monitoring points corresponding to the section at ZK243 + 291 were set in the model (Figure 9). The comparison between simulation values and monitoring values of the monitoring section is shown in Table 3. The average relative error is 10.20% and the maximum relative error is 13.31%, indicating that the simulation results and the field monitoring results are in good agreement.

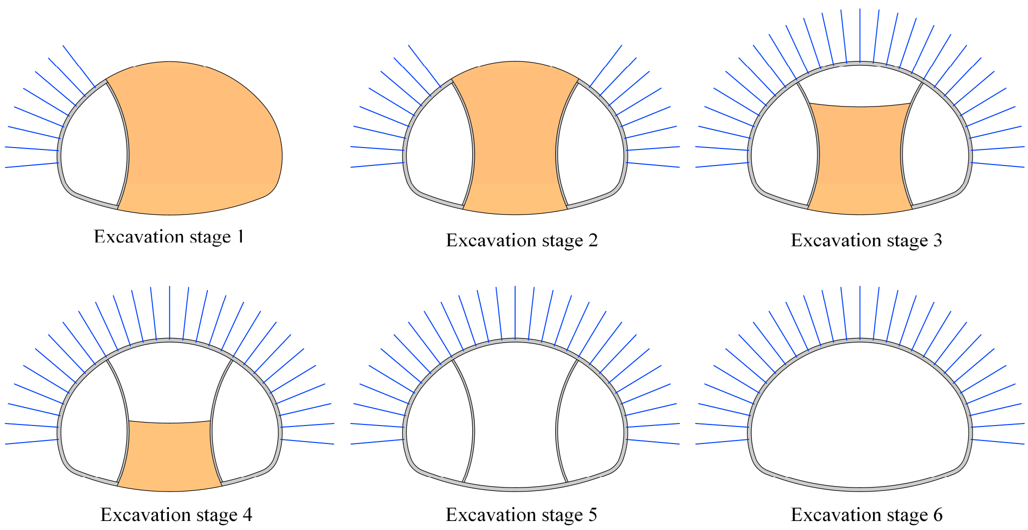

Figure 7. Schematic view of the excavation sequence of the twin-side heading method.

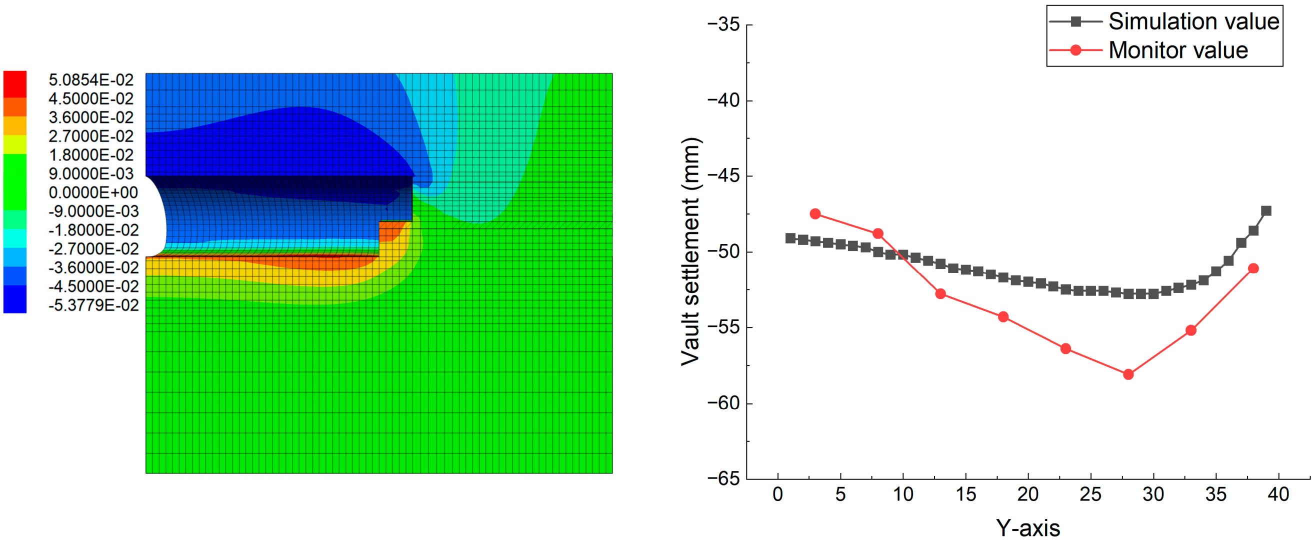

(**a**) (**b**)

Figure 8. Vertical displacement of the longitudinal section: (**a**) contour; (**b**) comparison between simulation value and monitoring value.

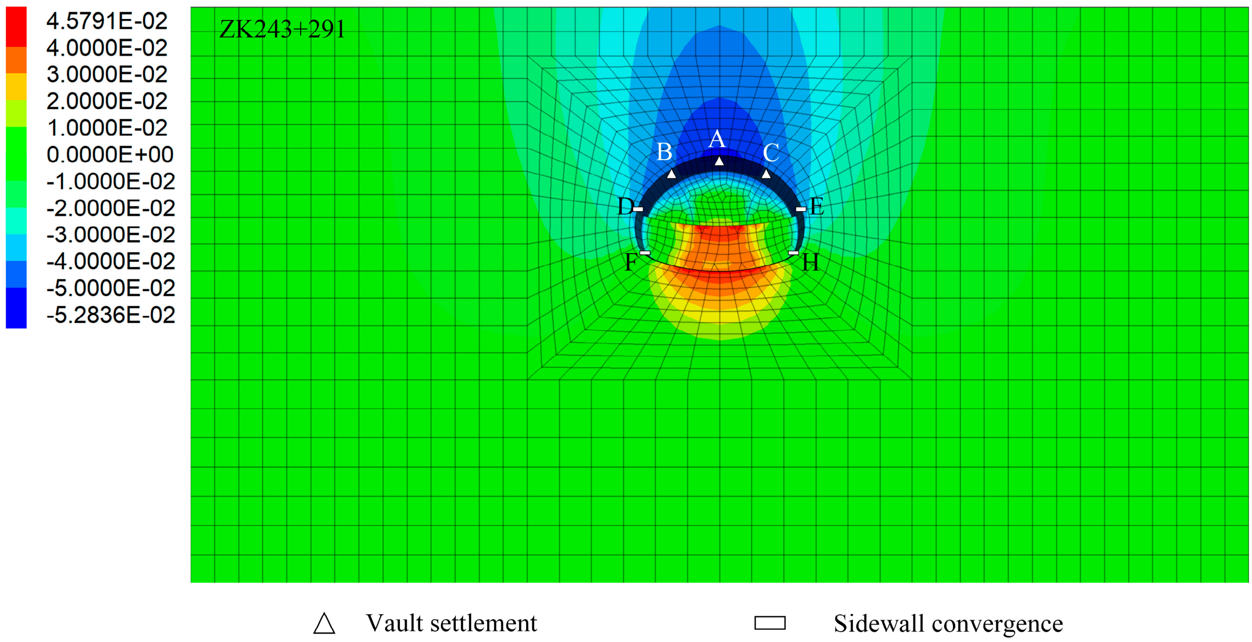

Figure 9. Vertical displacement contour and monitoring point layout at ZK243 + 291.

Table 3. Displacement of the monitoring section at ZK243 + 291.

Item	Vault Settlement			Sidewall Convergence	
	A	B	C	DE	FH
Simulation value (mm)	−52.8	−45.2	−45.4	−64.6	−87.6
Monitoring value (mm)	−58.1	−49.4	−51.1	−73.2	−92.7
Relative error (%)	10.04	9.29	12.56	13.31	5.82
Average relative error (%)			10.20		

3.3. Stability Analysis of the Surrounding Rock

Following the excavation and the support installation procedures for section A, section B was excavated by the three-bench method instead of the CRD method to expedite the construction schedule, with each bench measuring 5 m in length. At about 01:00 on 19 December 2019, excavation of the upper bench was completed for 5 m. Due to a shortage of cement, shotcrete construction, and rock bolt grouting did not begin until 12:40 and was completed at about 16:00. The collapse occurred at 19:40 p.m. (Figure 10).

Figure 10. Tunnel collapse.

3.3.1. Simulation Scheme

In order to analyze the stability of the tunnel, the strength reduction method was introduced into numerical simulations, and the construction process of the collapsed section (ZK243 + 279~ZK243 + 274) was simulated using the numerical model developed in Section 2. The construction process of the CRD method was simulated for comparison, and the installation time of the support system was taken into account.

Figure 11 shows the excavation models for the three-bench method and the CRD method based on the excavation sequence shown in Figure 12. The corresponding monitoring points, which were also selected as characteristic points, were set in the model. Both the three-bench method and the CRD method were set up with five construction cases, with 20%, 40%, 60%, 80%, and 90% stress release rates of the surrounding rock prior to the installation of the primary support, respectively. The case identifiers are listed in Table 4 for convenience.

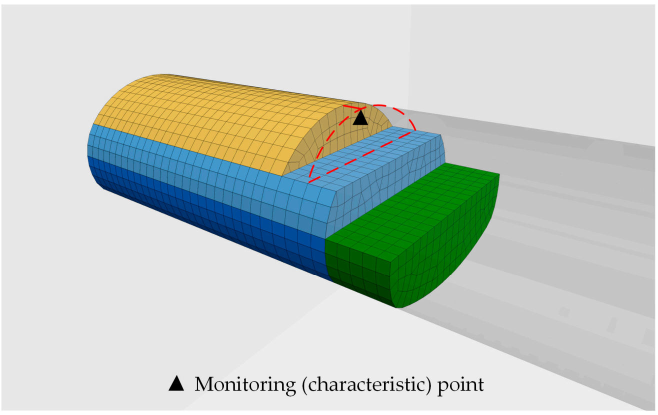

(**a**)

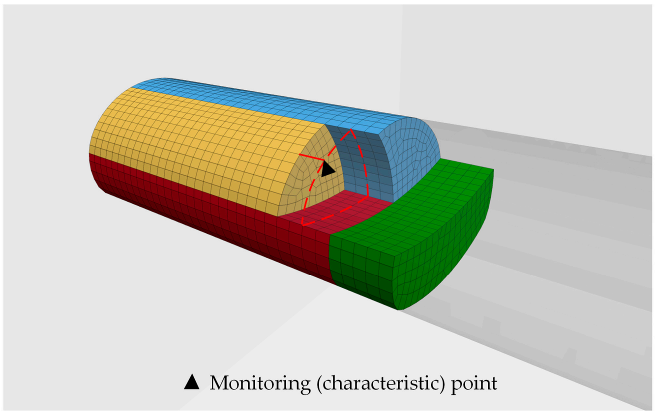

(**b**)

Figure 11. Excavation model: (**a**) three-bench method; (**b**) CRD method.

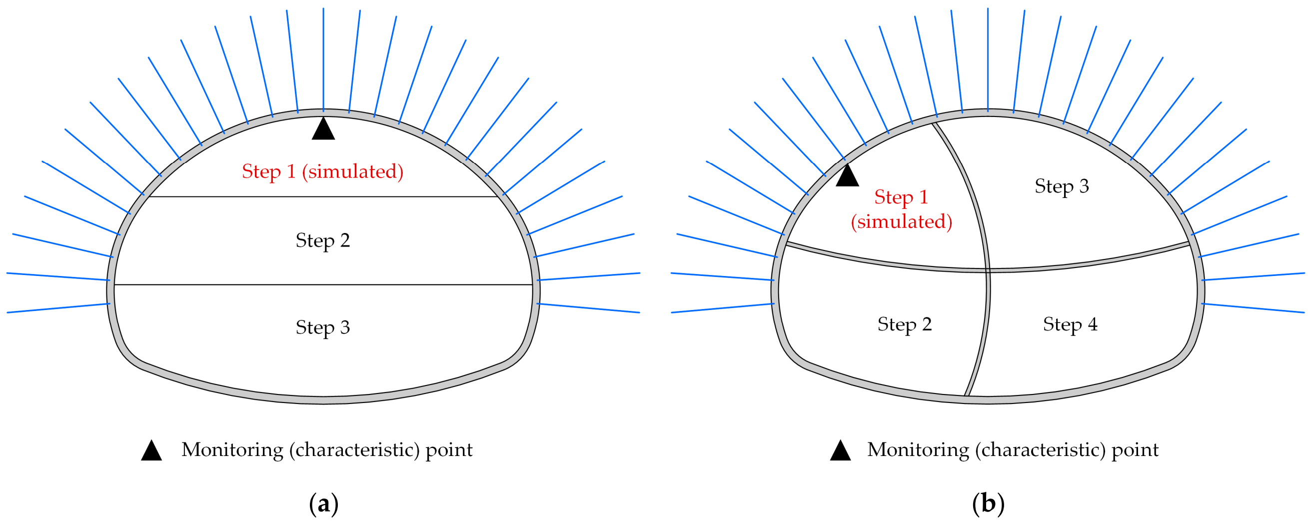

Figure 12. Diagram of excavation sequence: (**a**) three-bench method; (**b**) CRD method.

Table 4. Identifiers of construction cases.

Method	**Stress Release Rate (%)**				
	20	**40**	**60**	**80**	**90**
Three-bench	B1	B2	B3	B4	B5
CRD	C1	C2	C3	C4	C5

3.3.2. Calculation of Safety Factors

Derived from numerical simulations, the relationship curves between the displacements of the characteristic points and the reduction coefficients are shown in Figure 13. Determined by the displacement mutation criterion, the safety factors of the surrounding rock are shown in Figure 14.

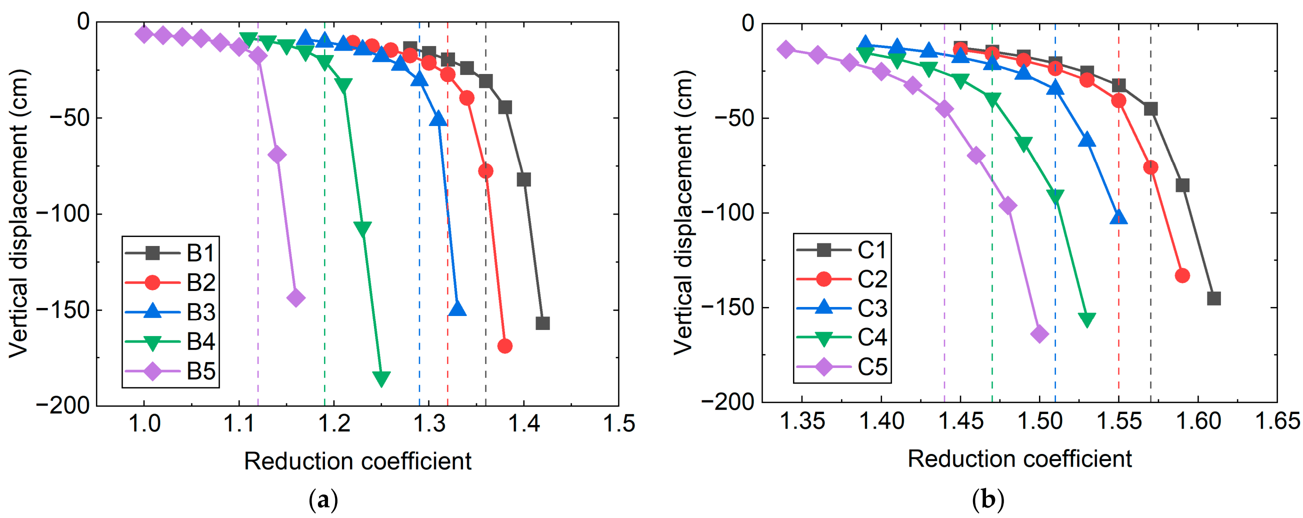

Figure 13. Evolution of the displacements of the characteristic points with the strength reduction coefficients: (**a**) three-bench method; (**b**) CRD method.

It is observed that the safety factor of the surrounding rock of the case excavated using the three-bench method is less than 1.30 when the stress release rate is greater than or equal to 60 percent, indicating that the tunnel is unstable and prone to collapse. In contrast, the five cases excavated using the CRD method have a safety factor greater than 1.30. In addition, changing the excavation method from CRD to three-bench reduces the safety factor of the surrounding rock, with the latter being significantly more affected by the support timing than the former.

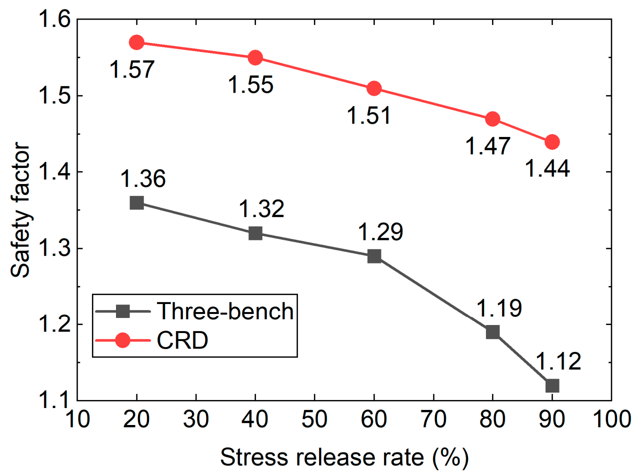

Figure 14. Variation of safety factor with stress release rate.

3.4. Generating Data Set

In this paper, the following assumptions were made in consideration of the actual conditions: (1) Due to the limited influence of stratum II on the construction and the highly developed manufacturing and construction techniques of the support system, the properties of the stratum II and the support system were assumed to be deterministic. (2) Stratum I, through which the tunnel passes, has a significant influence on the construction, so the uncertainty of stratum I was taken into account. (3) The safety factor of the surrounding rock is almost independent of elasticity modulus and Poisson's ratio but is mainly related to the shear strength [34]; therefore, the cohesion and the friction angle of stratum I were treated as random variables, which is consistent with the large variation of the shear parameters of geomaterials in practice. (4) The cohesion and the friction angle of stratum I followed the lognormal and normal distributions, respectively, and both were considered as independent variables. Table 5 shows the mean values and the coefficients of variation for the two random variables, which are based on the deterministic material values of stratum I in Table 1.

Table 5. Probabilistic characteristics of stratum I.

Variables	Mean	Cov	Probability Distribution Type
Cohesion (kPa)	10	0.2	Lognormal
Friction angle (°)	30	0.1	Normal

Several sampling methods are available to cover the multivariate space, including the inverse transform sampling method (ITM), Latin hypercube sampling (LHS), Halton sequence, and Sobol sequence [35]. In this paper, the LHS was used owing to its efficiency to stratify across the range of each sampled variable [36]. For each case, 100 random samples consisting of the two random variables were generated and introduced into the FLAC3D model to simulate the system responses and determine the safety factor of the surrounding rock. In this section, safety factors were determined by the abrupt displacement criterion as well. The data set used for training and testing the SVR model was then constructed with 100 input random samples stored as a 100×2 matrix and corresponding output safety factors stored as a 100-component vector (Figure 15).

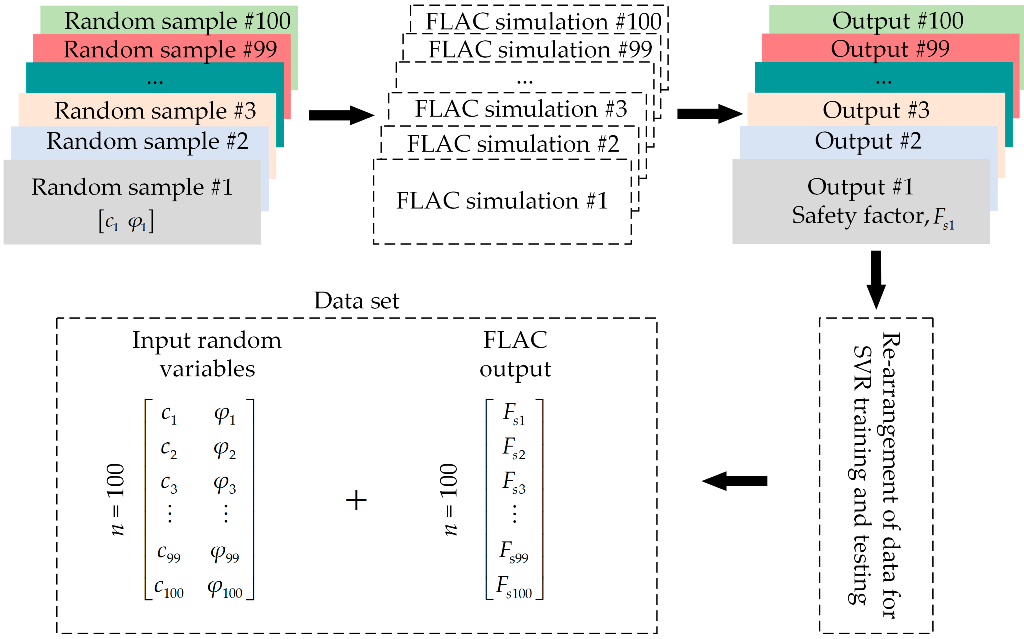

Figure 15. Schematic diagram of constructing data set for SVR training and testing.

3.5. SVR Training for Safety Factor Prediction

A well-trained SVR model will output the corresponding safety factor directly if a new random sample is input. The goal of the training process is to minimize the root mean square error (RMSE) of the SVR model. Using case B1 as an example, the corresponding data set was first normalized, i.e., all input and output variables were scaled between $[-1, 1]$ after the normalization process to eliminate differences in magnitude between variables. The normalized data set was then divided into a training set consisting of 80 random samples and a testing set consisting of 20 random samples. The optimal hyperparameters (C, γ) of the SVR model were then determined using the grid search method and the training set. Given the small sample size of the training set, fivefold cross-validation was performed. The search range for the optimal hyperparameters is $[2^{-10}, 2^{10}]$. As shown in Figure 16, each grid point in the logarithmic coordinates represents a pair of hyperparameters and the corresponding RMSE. When the hyperparameters C and γ were set to 32 and 0.03125, respectively, the RMSE was the minimum.

The SVR model for case B1 with the optimal hyperparameters, i.e., $(C, \gamma) = (32, 0.03125)$, was constructed, trained, and tested after the optimization procedure. Figure 17a shows a comparison between the training data and the output results of the SVR model, while Figure 17b shows the corresponding errors. There is a good agreement between the SVR outputs and the training data. The mean deviation and the standard deviation (StD) of the errors are relatively small, and the majority of the errors are close to zero (Figure 17c). The testing process of the SVR model shows the same phenomenon (Figure 18). It can be seen that the corresponding RMSE is close to 0 and the coefficient of determination R^2 is close to 1 for both the training and testing set. In addition, all the SVR outputs were plotted against their corresponding FLAC outputs, and the majority of the data points lie on the line of best fit with a slope of 1 (Figure 19). In conclusion, the constructed SVR model has demonstrated an ideal performance in predicting the safety factor of the surrounding rock.

Similarly, the optimal hyperparameters of the SVR models can be determined for the remaining cases, as shown in Table 6.

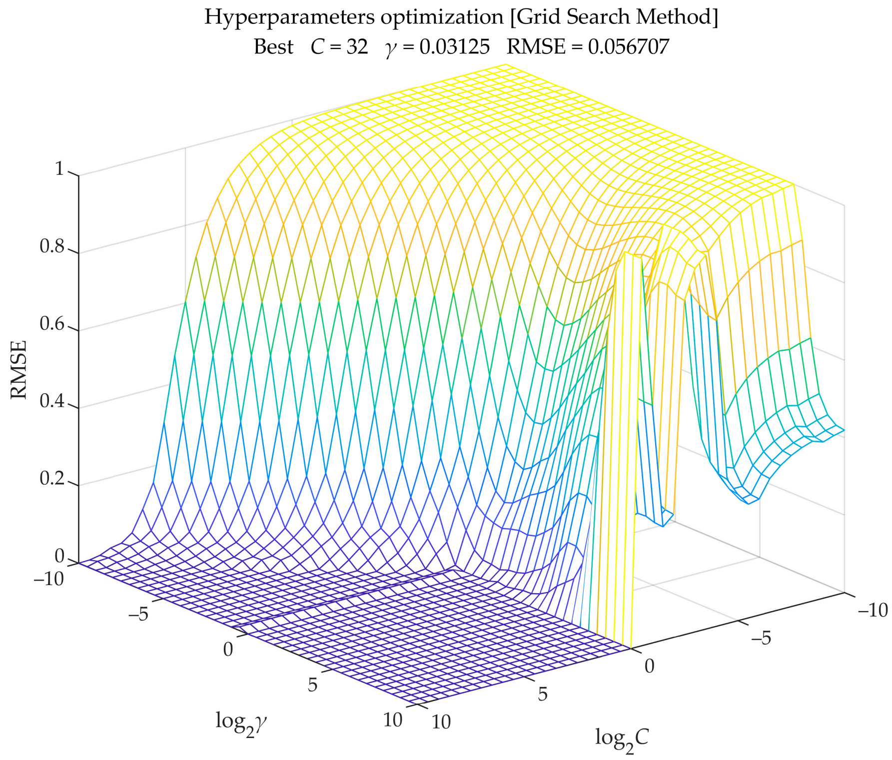

Figure 16. Optimization result of hyperparameters.

Table 6. Optimal hyperparameters for all cases.

Para-Meter	Three-Bench Method					CRD Method				
	B1	**B2**	**B3**	**B4**	**B5**	**C1**	**C2**	**C3**	**C4**	**C5**
C	32	16	11.314	128	45.256	22.627	5.566	16	8	8
γ	0.0313	0.0442	0.063	0.008	0.0313	0.044	0.088	0.044	0.063	0.088

3.6. Collapse Probability Calculation

In order to calculate the collapse probability, the reliability model was established and a limit state function was defined as follows:

$$g(X) = F_s(X) - F_{s0} \tag{9}$$

where $F_s(\bullet)$ = safety factor obtained from the SVR as a function of the input random variables $X = \{(c_1, \varphi_1), (c_2, \varphi_2), \ldots, (c_N, \varphi_N)\}^T$; and $F_{s0} = 1.30$ is the safety factor threshold in this paper. The occurrence of $g(X) < 0$ indicates that the prediction of the SVR exceeds the threshold value. Therefore, the collapse probability p_c can be defined as follows:

$$p_c = P(g(X) < 0) = P(F_s(X) < F_{s0}) \approx \frac{k}{N} \tag{10}$$

where k is the number of random samples that fall into the failure domain.

Before implementing the MC simulation with the well-trained SVR model, it is critical to ensure that the number of samples used in the MC simulation is sufficient so that the resulting probability does not change significantly as more samples are added. For this purpose, using case B1 as an illustration, the values of probability p_c were calculated using different numbers of random samples and then plotted on a graph to show the convergence process (Figure 20). The result indicates that the probability convergence in the MC simulation can be guaranteed if the sample size exceeds 10,000. In this paper, 500,000 random samples were used in the MC simulation.

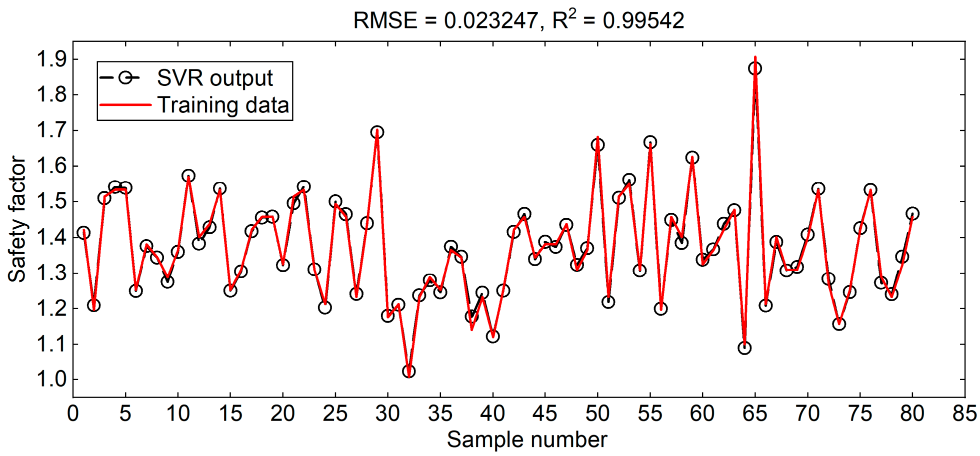

(**a**)

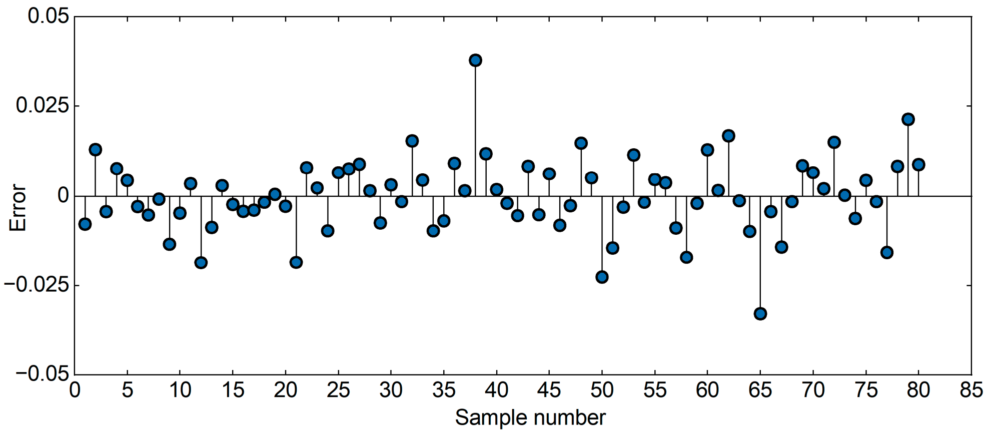

(**b**)

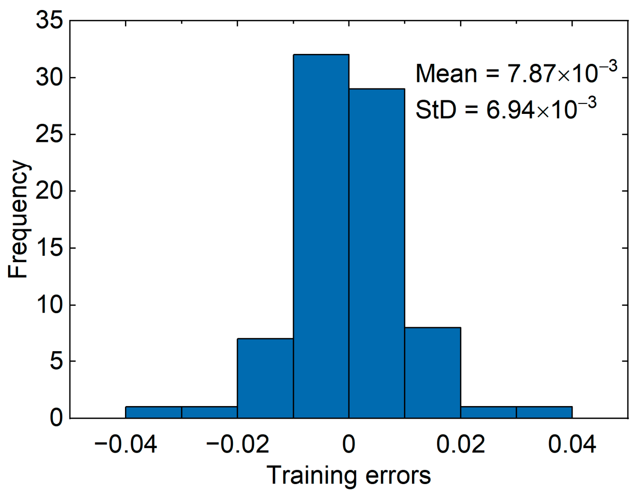

(**c**)

Figure 17. Predictive performance of the training set: (**a**) SVR output versus FLAC output; (**b**) error; (**c**) histogram of error.

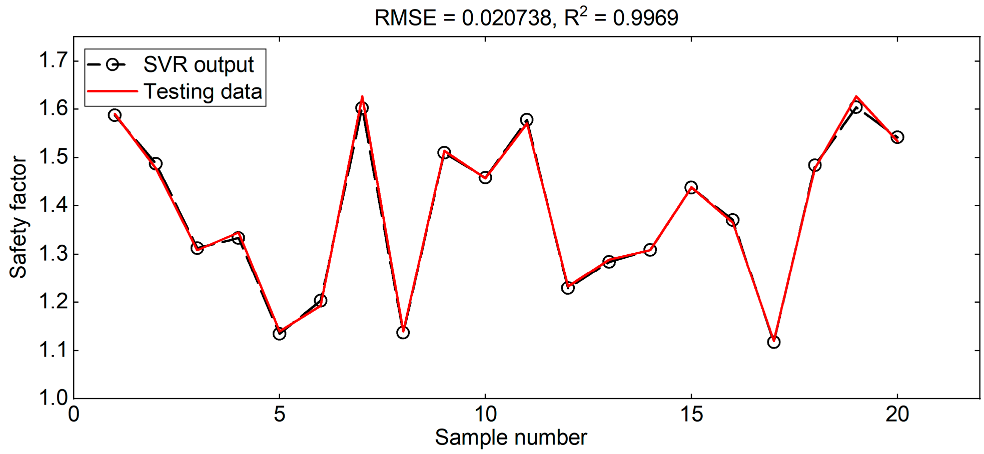

(**a**)

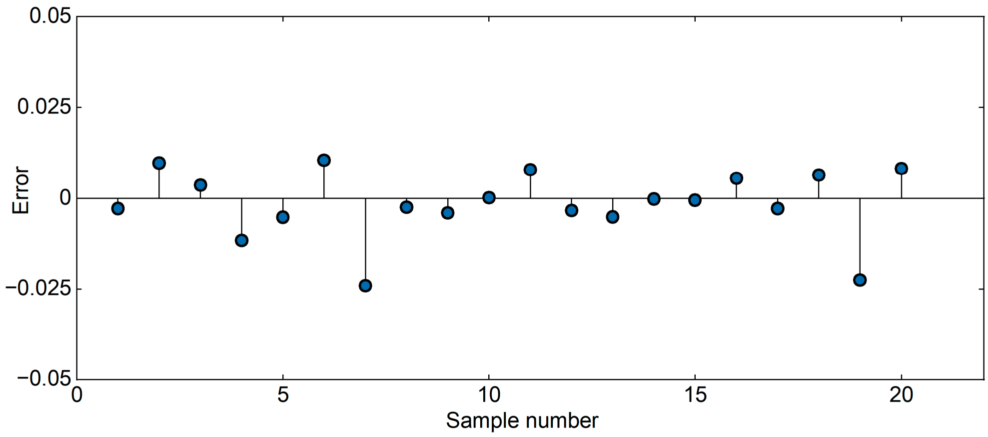

(**b**)

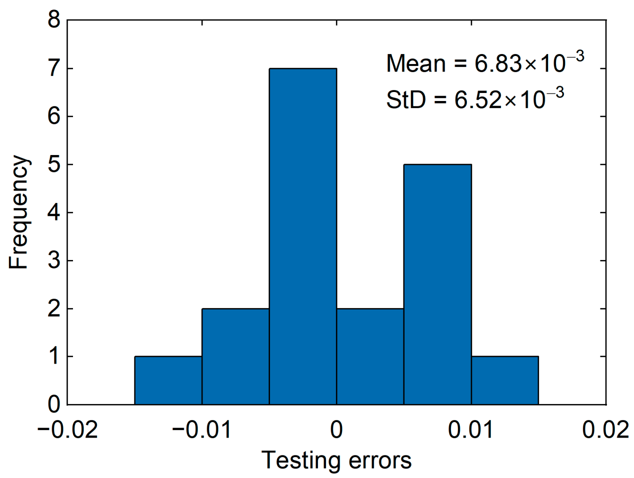

(**c**)

Figure 18. Predictive performance of the testing set: (**a**) SVR output versus FLAC output; (**b**) error; (**c**) histogram of error.

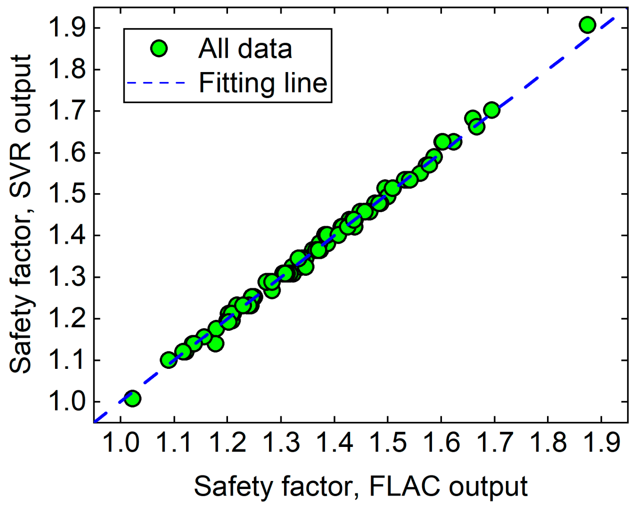

Figure 19. SVR predictions against simulation results for all data.

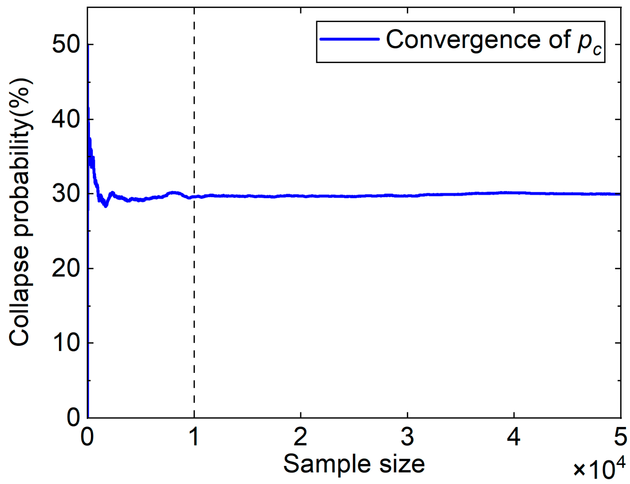

Figure 20. Convergence process of the Monte Carlo simulation.

Figure 21 shows the histogram of the safety factor of case B1 obtained from the SVR model in the MC simulation. Spearman's rank correlation coefficient was used to show the efficiency of each input random variable on the safety factor, as illustrated in Table 7. The result indicates that the efficiency of cohesion is greater than the friction angle in this study.

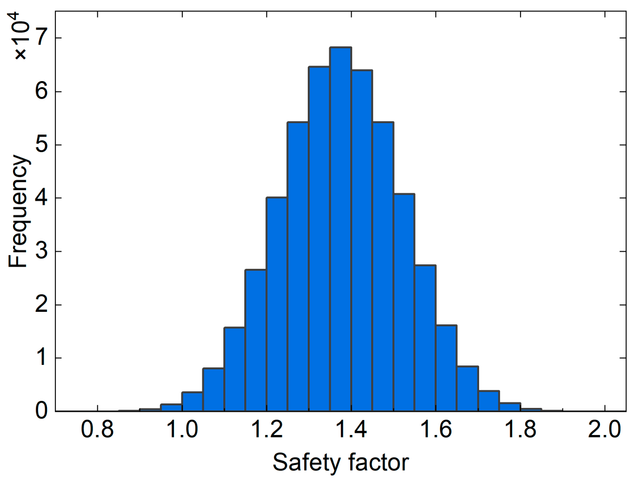

Figure 21. Histogram of the safety factor of case B1 obtained from the SVR model.

Table 7. Spearman's rank correlation coefficient of each input variable.

Input Random Variable	Cohesion	Friction Angle
Spearman's rank correlation coefficient	0.7741	0.5962

Then, the collapse probabilities in all cases were calculated, and the variation of collapse probabilities with stress release rates for the two excavation methods is shown in Figure 22.

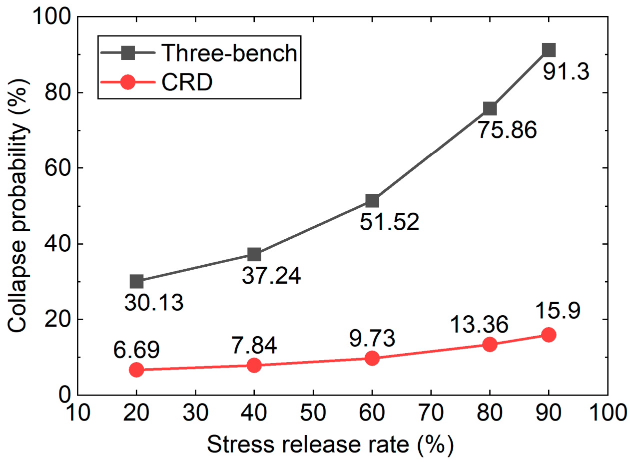

Figure 22. Collapse probability versus stress release rate.

3.7. Result Analysis and Validation

The Jinzhupa Tunnel is a super-large section tunnel, and the surrounding rock through which the left tunnel passes consists of fragmented, strongly weathered shale, which is very poor in self-stability. The CRD method increases the excavation height compared with the three-bench method but significantly reduces the excavation span, resulting in less disturbance to the surrounding rock. In addition, when the support system is installed, the temporary support measure, which consists of the middle wall and the temporary invert, more effectively limits the displacement evolution of the surrounding rock. Therefore, the collapse probabilities of the CRD-excavated cases, which are less than 16%, are significantly lower than those of the three-bench method. In addition, the collapse probability gradually increases as the support timing is gradually delayed. In contrast, the collapse probabilities of the cases excavated using the three-bench method are all greater than 30%, and the collapse probability increases sharply as the support timing is gradually delayed. In addition, the collapse probability exceeds 50% when the stress release rate of the surrounding rock is 60% or higher, and it reaches 91.30% when the stress release rate is 90%.

In conclusion, using the three-bench method to excavate the tunnel is riskier than using the CRD method, and the stability of the surrounding rock and the tunnel cannot be guaranteed if the support system is not installed in time. The results indicate that the field collapse was caused by the change from the CRD method to the three-bench method without additional ground-reinforcement measures and the very late installation of supports. The same but qualitative conclusion of the collapse causes can be obtained from the collapse analysis report provided by the project manager, which verifies the reliability of the proposed method.

4. Discussion

Unlike the results of a qualitative risk assessment, which are risk levels, risk probabilities are quantitative and more intuitive. The proposed method can calculate the collapse risk probabilities for mountain tunnels under specific construction behaviors, which provides an intuitive reference for project managers to choose a safe excavation method and to develop a reasonable construction scheme.

In this study, the numerical method was used to determine the stability of the tunnel, which makes the results of the collapse risk assessment more objective. The safety factor of the surrounding rock was chosen as the output random variable; the reliability index was chosen instead of the deformation as the former is sometimes more reliable because the deformation is significantly related to the deformation modulus, and the actual deformation modulus is difficult to determine.

Machine-learning techniques such as support vector regression can significantly increase computational efficiency. In this study, FLAC3D simulations, SVR training, testing, and prediction were performed on a workstation configured with 256 GB of RAM, two Intel Xeon Platinum 8268 processors, and an Nvidia GeForce GTX 1070 GPU. Table 8 compares the time required by the FLAC3D simulation method and the SVR algorithm to output the same number of safety factors. The FLAC3D simulation method required approximately 345,600 s to complete the assignment of 100 samples, while the SVR algorithm required less than 1 s. Thus, the SVR algorithm is considerably more efficient than the FLAC3D simulation method. Since at least 10,000 samples are required, it is impractical to calculate the collapse probability using the MC method without the SVR algorithm.

Table 8. Comparison of the time consumption between the SVR algorithm and the FLAC3D simulation method for outputting safety factors.

Method	100 Samples (s)	10,000 Samples (s)	500,000 Samples (s)
FLAC3D	345600	—	—
SVR	0.012	0.018	0.214

This study still has some limitations. First, the loss of the collapse, which is an important part of the assessment result as well, cannot be obtained by the proposed method. Second, the support installation timing was controlled by an approximate approach, i.e., the stress release method, which is somewhat different from the actual excavation. Third, some unaccounted-for factors may influence the result of tunnel stability analysis and collapse probability. For instance, the correlation between cohesion and friction angle was not considered in this study. Finally, the proposed method does not include the dynamics or fluid mechanics method, so it cannot be applied to other tunnel projects under any complex conditions, such as vibration from vehicles and machines, earthquakes, and developed groundwater. However, the ideas of this study will be helpful if the necessary risk factors are considered and the appropriate methods are implemented.

5. Conclusions

By introducing the reliability theory, this paper proposes a novel collapse probability prediction method based on numerical simulation, support vector regression (SVR), and the Monte Carlo (MC) method in order to overcome the subjectivity and lack of probability quantification in existing risk assessment methods for tunnel collapse. The Jinzhupa Tunnel was used to illustrate the process of the proposed method. The strength reduction method, which provides an effective way to analyze the stability of the tunnel, was introduced into the FLAC3D simulation to calculate the safety factor of the surrounding rock. By defining the shear strength parameters of the surrounding rock as random variables, the problem was formulated as a reliability model. The SVR model was then trained to represent a nonlinear mapping between the shear parameters and the safety factor. The computational efficiency was significantly increased by substituting the FLAC3D simulation with a well-trained SVR model. Finally, in conjunction with the well-trained SVR model, a sufficient number of random samples were used to calculate the collapse probability using the MC method. The results show that using the three-bench method to excavate the tunnel is riskier than using the CRD method, and the stability of the surrounding rock and the tunnel cannot be guaranteed if the support system is not installed in time. As the result was in good agreement with the collapse analysis report, the feasibility and the reliability of the proposed method were verified, indicating that the method can be used to predict the probability of collapse in a practical risk assessment of mountain tunnel construction.

Author Contributions: Conceptualization, H.L., G.L., H.Y. and Y.Z.; methodology, H.L.; software, H.L.; validation, G.L.; investigation, H.Y. and Y.Z.; resources, G.M. and B.W.; data curation: G.L.; writing—original draft preparation, H.L.; writing—review and editing, G.M., H.L. and B.W.; visualization, H.Y. and Y.Z.; supervision, G.M. and B.W.; funding acquisition, G.M. All authors have read and agreed to the published version of the manuscript.

Funding: This research was funded by the National Natural Science Foundation of China, grant number 52208389.

Institutional Review Board Statement: Not applicable.

Informed Consent Statement: Not applicable.

Data Availability Statement: The data presented in this study are available upon request from the corresponding author.

Conflicts of Interest: The authors declare no conflict of interest. The funders had no role in the design of the study; in the collection, analyses, or interpretation of data; in the writing of the manuscript; or in the decision to publish the results.

References

1. Hong, K.R.; Feng, H.H. Development Trends and Views of Highway Tunnels in China over the Past Decade. *China J. Highw. Transp.* **2020**, *33*, 62–76.
2. Wang, X.L.; Lai, J.X.; Qiu, J.L.; Xu, W.; Wang, L.X.; Luo, Y.B. Geohazards, reflection and challenges in Mountain tunnel construction of China: A data collection from 2002 to 2018. *Geomat. Nat. Hazards Risk* **2020**, *11*, 766–785. [CrossRef]
3. Ou, G.; Jiao, Y.; Zhang, G.; Zou, J.; Tan, F.; Zhang, W. Collapse risk assessment of deep-buried tunnel during construction and its application. *Tunn. Undergr. Space Technol.* **2021**, *115*, 104019. [CrossRef]
4. Xu, Z.G.; Cai, N.G.; Li, X.F.; Xian, M.T.; Dong, T.W. Risk assessment of loess tunnel collapse during construction based on an attribute recognition model. *Bull. Eng. Geol. Environ.* **2021**, *80*, 6205–6220. [CrossRef]
5. Sharafat, A.; Latif, K.; Seo, J. Risk analysis of TBM tunneling projects based on generic bow-tie risk analysis approach in difficult ground conditions. *Tunn. Undergr. Space Technol.* **2021**, *111*, 103860. [CrossRef]
6. Sun, J.L.; Liu, B.G.; Chu, Z.F.; Chen, L.; Li, X. Tunnel collapse risk assessment based on multistate fuzzy Bayesian networks. *Qual. Reliab. Eng. Int.* **2018**, *34*, 1646–1662. [CrossRef]
7. Ou, X.D.; Wu, Y.F.; Wu, B.; Jiang, J.; Qiu, W.X. Dynamic Bayesian Network for Predicting Tunnel-Collapse Risk in the Case of Incomplete Data. *J. Perform. Constr. Facil.* **2022**, *36*, 04022034. [CrossRef]
8. Li, F.Y. Research on Tunnel Collapse Risk Prediction and Control. Master's Thesis, Central South University, Changsha, China, 2011.
9. Wu, B.; Qiu, W.X.; Huang, W.; Meng, G.W.; Nong, Y.; Huang, J.S. A Multi-Source Information Fusion Evaluation Method for the Tunneling Collapse Disaster Based on the Artificial Intelligence Deformation Prediction. *Arab. J. Sci. Eng.* **2022**, *47*, 5053–5071. [CrossRef]
10. Paternesi, A.; Schweiger, H.F.; Scarpelli, G. Numerical analyses of stability and deformation behavior of reinforced and unreinforced tunnel faces. *Comput. Geotech.* **2017**, *88*, 256–266. [CrossRef]
11. Hu, X.Y.; Fu, W.; Wu, S.Z.; Fang, Y.; Wang, J.; He, C. Numerical study on the tunnel stability in granular soil using DEM virtual air bag model. *Acta Geotech.* **2021**, *16*, 3285–3300. [CrossRef]
12. Yu, W.B.; Zhang, T.Q.; Lu, Y.; Han, F.L.; Zhou, Y.F.; Hu, D. Engineering risk analysis in cold regions: State of the art and perspectives. *Cold Reg. Sci. Technol.* **2020**, *171*, 102963. [CrossRef]
13. Xiong, Z.M.; Lu, H.; Wang, M.Y.; Qian, Q.H.; Rong, X.L. Research progress on safety risk management for large scale geotechnical engineering construction in China. *Rock Soil Mech.* **2018**, *39*, 3703–3716. [CrossRef]
14. Wu, Y.X.; Bao, H.; Wang, J.C.; Gao, Y.F. Probabilistic analysis of tunnel convergence on spatially variable soil: The importance of distribution type of soil properties. *Tunn. Undergr. Space Technol.* **2021**, *109*, 103747. [CrossRef]
15. Tran, T.T.; Salman, K.; Han, S.R.; Kim, D. Probabilistic Models for Uncertainty Quantification of Soil Properties on Site Response Analysis. *ASCE-ASME J. Risk Uncertain. Eng. Syst. Part A Civ. Eng.* **2020**, *6*, 04020030. [CrossRef]
16. Elbaz, K.; Yan, T.; Zhou, A.; Shen, S. Deep learning analysis for energy consumption of shield tunneling machine drive system. *Tunn. Undergr. Space Technol.* **2022**, *123*, 104405. [CrossRef]
17. Elbaz, K.; Zhou, A.; Shen, S. Deep reinforcement learning approach to optimize the driving performance of shield tunnelling machines. *Tunn. Undergr. Space Technol.* **2023**, *136*, 105104. [CrossRef]

18. Tiwari, G.; Pandit, B.; Latha, G.M.; Sivakumar Babu, G.L. Probabilistic analysis of tunnels considering uncertainty in peak and post-peak strength parameters. *Tunn. Undergr. Space Technol.* **2017**, *70*, 375–387. [CrossRef]
19. Zhou, M.; Shadabfar, M.; Xue, Y.; Zhang, Y.; Huang, H. Probabilistic Analysis of Tunnel Roof Deflection under Sequential Excavation Using ANN-Based Monte Carlo Simulation and Simplified Reliability Approach. *ASCE-ASME J. Risk Uncertain. Eng. Syst. Part A Civ. Eng.* **2021**, *7*, 4021043. [CrossRef]
20. Yang, X.; Huang, F. Stability analysis of shallow tunnels subjected to seepage with strength reduction theory. *J. Cent. South Univ. Technol.* **2009**, *16*, 1001–1005. [CrossRef]
21. Xia, C.C.; Xu, C.B.; Zhao, X. Study of the Strength Reduction DDA Method and Its Application To Mountain Tunnel. *Int. J. Comp. Methods* **2012**, *9*, 1250041. [CrossRef]
22. Shiau, J.; Al-Asadi, F. Stability analysis of twin circular tunnels using shear strength reduction method. *Geotech. Lett.* **2020**, *10*, 311–319. [CrossRef]
23. Zhou, P.; Jiang, Y.; Zhou, F.; Gong, L.; Qiu, W.; Yu, J. Stability Evaluation Method and Support Structure Optimization of Weak and Fractured Slate Tunnel. *Rock Mech. Rock Eng.* **2022**, *55*, 6425–6444. [CrossRef]
24. Zhang, L.M.; Zheng, Y.R.; Wang, Z.Q.; Wang, J.X. Application of strength reduction finite element method to road tunnels. *Rock Soil Mech.* **2007**, *28*, 97–101, 106.
25. Jiang, Q.; Feng, X.; Xiang, T. Discussion on method for calculating general safety factor of underground caverns based on strength reduction theory. *Rock Soil Mech.* **2009**, *30*, 2483–2488. [CrossRef]
26. Abi, E.; Zheng, Y.R.; Feng, X.T.; Xiang, Y.Z. Study of the Safety Factor for Tunnel Stability Considering the Stress Release Effect. *Mod. Tunn. Technol.* **2016**, *53*, 70–76. [CrossRef]
27. Li, J.; Si, J.L.; Zhong, H.; Zhao, R.W. A study of the rock mass stability of two-tube large-span tunnels based on strength reduction method. *China Civ. Eng. J.* **2017**, *50*, 198–202. [CrossRef]
28. Zhang, C.Q.; Feng, X.T.; Zhou, H.; Huang, S.L. Study of some problems about application of stress release method to tunnel excavation simulation. *Rock Soil Mech.* **2008**, *29*, 1174–1180.
29. Duncan, J.M.; Dunlop, P. Slopes in Stiff-Fissured Clays and Shales. *J. Soil Mech. Found. Div.* **1969**, *95*, 467–492. [CrossRef]
30. Chang, C.; Lin, C. LIBSVM: A Library for Support Vector Machines. *ACM Trans. Intell. Syst. Technol.* **2011**, *2*, 1–27. [CrossRef]
31. Vapnik, V. *Statistical Learning Theory*; Wiley: New York, NY, USA, 1998; Volume 10.
32. Zhou, C.; Yin, K.L.; Cao, Y.; Ahmed, B. Application of time series analysis and PSO–SVM model in predicting the Bazimen landslide in the Three Gorges Reservoir, China. *Eng. Geol.* **2016**, *204*, 108–120. [CrossRef]
33. Patle, A.; Chouhan, D.S. SVM Kernel Functions for Classification. In Proceedings of the 2013 International Conference on Advances in Technology and Engineering (ICATE), Mumbai, India, 23–25 January 2013; pp. 1–9. [CrossRef]
34. Zheng, Y.R.; Qiu, C.Y.; Zhang, H.; Wang, Q.Y. Exploration of stability analysis methods for surrounding rocks of soil tunnel. *Chin. J. Rock Mech. Eng.* **2008**, *27*, 1968–1980.
35. Zio, E. *The Monte Carlo Simulation Method for System Reliability and Risk Analysis*; Springer: Berlin/Heidelberg, Germany, 2013.
36. Helton, J.C.; Davis, F.J. Latin hypercube sampling and the propagation of uncertainty in analyses of complex systems. *Reliab. Eng. Syst. Safe* **2003**, *81*, 23–69. [CrossRef]